Computer-Aided Visual Analysis of Feathers

Jessica R. Baron[1], Pepper W. Trail[2], and Eric K. Patterson[1]

[1]Clemson University, North Charleston, SC, USA
Email: {jrbaron, ekp}@clemson.edu

[2]U.S. Fish & Wildlife Service, National Fish and Wildlife Forensic Laboratory, Ashland, OR, USA
Email: pepper_trail@fws.gov

***Abstract*—Feathers are fascinating natural components of birds and other, extinct dinosaurs. They exhibit a variety of crucial biological properties that are studied in multiple fields. Here we present work in visual analysis of feathers that leverages image-processing methods to observe important physical data about the structure and shape of feathers. Such data may be used to inform ornithology or paleontology as well as used to synthesize accurate computerized representations of feathers for high-fidelity visualization and interactive rendering.**

I. Introduction

The feathers of birds and other dinosaurs are studied in ornithology and paleontology. A variety of other fields also seek understanding of properties of feathers such as their strength, aerodynamics, coloration, and insulation in order to inform material design and other applications [1] [2]. Additionally, visualizations of feathers are needed for accurate scientific materials, and feathers are often modeled as a major visual aspect for characters in cinema and gaming. Here we present novel, ongoing work in visual analysis of feathers and describe methods that we have developed for extracting physical properties from images of feathers. Although these techniques could be employed using any photographs of feathers, the primary source of images used for this work is The Feather Atlas [3]. It consists of a well-cataloged library of images of flight feathers from various types of birds throughout North America, images selected from the curated collection of the National Fish and Wildlife Forensics Laboratory.

II. Biological Background

Feathers are studied across disciplines such as ornithology, paleontology, physics, material science, and visual computing. This is particularly due to their unique, hierarchical structure. Figure 1 is an image of a feather taken with a scanning electron microscope (SEM) with several key substructures highlighted. A feather consists of a central shaft (blue in Figure 1) and two vanes composed entirely of barbs (yellow) branching from the rachis portion of the shaft (the bare portion is called the calamus). A single barb is composed of a centered ramus (dark center of the yellow portion) and many barbules (green and red). Pennaceous barbs as pictured are connected together via their barbules. These barbules are either distal (green) or proximal (red). Distal barbules own hooklets that connect with rods on the adjacent proximal barbules. Six main types of feathers exist which vary in function, placement, and anatomical composition [4]. We focus on flight feathers (primaries and secondaries on the wing and rectrices on the tail) due to their visibility, shape, and the available data, but the techniques presented can be applied for the other types.

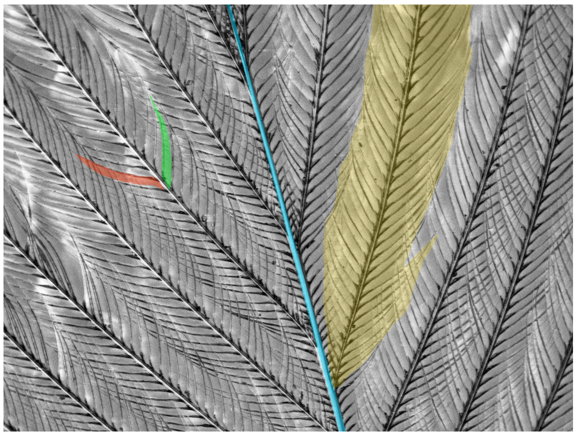

Fig. 1: SEM image of a feather with the shaft (blue), a barb (yellow), a distal barbule (green), and a proximal barbule (red) highlighted.

III. Related Work

A. Visual Computing

Concerning feather geometry for computer graphics, several works focus on curved-based procedural feather generation but do not use statistics of real-world feathers as a basis [11], [12], [13], [14], [15], [16], [17]. Some image processing has been applied to the feather-processing industry in denoising SEM captures of feathers [18] and extracting the general shapes of the shaft and vanes in feather images [19]. Another study links 2D image processing and 3D geometry generation of

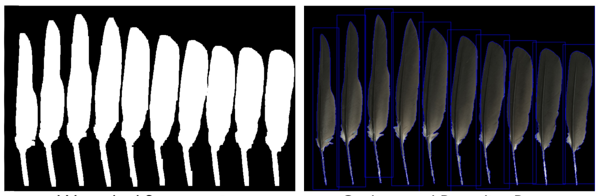

Fig. 2: Image segmentation using the Watershed algorithm of multi-feather scans from the Feather Atlas.

Data Summary from Ornithological Studies					
Attribute	Feather Type(s)	Bird(s)	Value	Unit	Reference
Barb Angle	3 Primaries	60 Species	5-50	degrees	Feo, Field, & Prum [5]
Barb Angle	Covert, Rectrex	Parrots	10-40	degrees	Feo & Prum [6]
Barb Length	3 Primaries	60 Species	10-60	mm	Feo, Field, & Prum [5]
Barb Length	Covert, Rectrex	Parrots	5-25	mm	Feo & Prum [6]
Vane Width	Covert, Rectrex	Parrots	5-15	mm	Feo & Prum [6]
Barb Diameter	Contour	Ducks, Cormorants	56	μm	Rijke [7]
Barb Spacing	Contour	Ducks, Cormorants	271	μm	Rijke [7]
Barbule Angle	unknown	Hummingbirds	0-70	degrees	Greenewalt [8]
Barbule Length	unknown	Hummingbirds	100	mm	Greenewalt [8]
Barbule Diameter	unknown	Hummingbirds	15	mm	Greenewalt [8]
Penn. Barb Density	Contour	Tits	1.47	per mm	Broggi et al. [9]
Penn. Barbule Density	Contour	Tits	2.17	per 0.1mm	Broggi et al. [9]
Rachis Cross Section	2 Primaries	Common Buzzard	0.03-5.79 x 0.01-3.47	mm^4	Osvath et al. [10]
Rachis Cross Section	2 Primaries	White Stork	0.14-26.1 x 0.08-22.3	mm^4	Osvath et al. [10]
Rachis Cross Section	2 Primaries	House Sparrow	0.40-42.6 x 0.10-24.8	μm^4	Osvath et al. [10]
Rachis Cross Section	2 Primaries	Pygmy Cormorant	5.00-55.0 x 4.00-55.8	μm^4	Osvath et al. [10]

TABLE I: A summary sample of related data manually gathered in ornithological studies.

feathers using landmark- and curve-based techniques which the techniques proposed in this paper build upon [20].

B. *Ornithological Studies*

Although visual-computing applications have not used data from real-world feathers, ornithological studies provide some insight into gathering statistics on the variation of feather shape. Most of the statistics found across these works is summarized in Table I including studying vane asymmetry for flight concerning barb angles and lengths [6], [5], water repellency concerning barb diameters and spacing [7], insulation concerning barb and barbule densities [9], iridescence based on barbule angles [8]. A recent study investigates the cross-sectional shape of the rachis of flight feathers sampled from birds with different patterns of flight. Measurements of the cross sections were manually taken as the second moment of area [10]; some of these results are in the last four rows of Table I shown as ranges of minimum and maximum values on single feathers. Other studies consider the nanoscopic arrangements within feathers using SEM and transmission electron microscopy (TEM) imagery for observing feather growth and iridescence [21] [22].

The measurements in these studies were all taken manually. In the next section we present methods for automating the analysis of feather images with particular focus on barb density and guiding curves.

IV. Method and Implementation

The proposed implementation involves data collection and automated visual analysis in order to extract information that describes the shapes of feathers. This study focuses on applying such data to drive generation of procedural feather geometry, but measurements and statistics of feather shapes may also be of interest across disciplines to further the understanding of these unique, organic structures.

The overall goal is to extract several important physical measurements from real feathers. We do this in a multi-step process by segmenting images of multiple, related feathers photographed together; approximating the number of barbs in a vane of each individual feather; and fitting curves to the various substructures that help define the specific shapes of each feather.

Our analysis begins with reading and leveraging meta-data from the Feather Atlas [3]. This data is associated with each single image containing multiple feathers of the same type taken from a single avian specimen. An example of a scan is shown in Figure 2 (with located bounding boxes drawn over it). To represent a variety of birds, samples from the Atlas were chosen based on taxonomic order. The Watershed algorithm is applied initially to segment the Feather Atlas scan into single-feather images as depicted in Figure 2; bounding boxes were expanded to ensure that the calamus was included with each single-feather image. Further image analysis is then applied to each split image on a per-feather basis. The shaft may be important to some analysis and could be found using landmark-based curve regression, image masks, or cross-correlation starting near the calamus.

To estimate barb density, we apply the Fast-Fourier Transform (FFT) algorithm to span of a vane in the individual feather images. A column of pixels along the center of a vane is selected as input for the FFT by searching the image space of the bounding box. The pixel count of the highest energy frequency divided by the vane's length in pixels yields the spacing between barbs in pixels. This value is then scaled by the actual vane length provided by the Feather Atlas data in order to derive a final barb density per millimeter of the vane. This technique is performed over a variety of feather samples and plotted in Figure 6. Figure 3 displays the column on the vane with red and blue alternating colors to show the barb sampling (left image) and a plot of the FFT values as barb counts in the vane (right).

We also investigate estimating the curvature of individual barbs, shown in Figure 4. This technique is a work in progress towards extracting guide splines that describe the curvature of barbs. Tracing a barb curve begins on the rachis portion of the shaft. A window of pixels in this area (window size relative to the resolution of a feather image) is selected to compare with neighboring matrices moving outwards from the shaft to the contour of the vane. The highest cross-correlation values among nearby windows, progressing horizontally by one pixel, determines which pixel area is chosen next until the border of the feather is met. These pixel locations can then be regressed in order to derive control vertices for the guide splines.

The landmark-based approach according to [20] is currently employed to process parametric curves for defining the general shape of the shaft and vane outlines as depicted in Figure 5. We are continuing use of the cross-correlation technique to find the shaft curvature without landmarks. Once this is known, barb angles (rotated orientations in respect to the shaft orientation) can be derived based on the shaft and barb as parameterized curves fitted from the trace.

V. Discussion and Conclusion

The main novel contribution of this study is the introduction of methods for visual analysis to derive values for barb density and provide a means to extract the curved shape of barbs. Figure 6 plots estimated numbers of barbs per millimeter of feather vanes. 102 feathers were sampled from the Feather Atlas from a variety of bird taxonomic orders and feather types.

The mean barb density of each type of flight feather is between 2.0 and 2.5 barbs per millimeter; this is similar to the measurement of 1.47 barbs per millimeter on contour feathers found in [9]. For comparison, we manually counted the barbs in several feather images and found most to be estimated accurately by the technique described here; however, in some images where lighting conditions and resolution are not sufficient for visual distinction, estimated counts were below the manually counted number. This is likely primarily due to a low visual sampling frequency as well as combined effects from the barb angle decreasing toward the distal end of the feather, particularly relative to lighting angle. If lighting

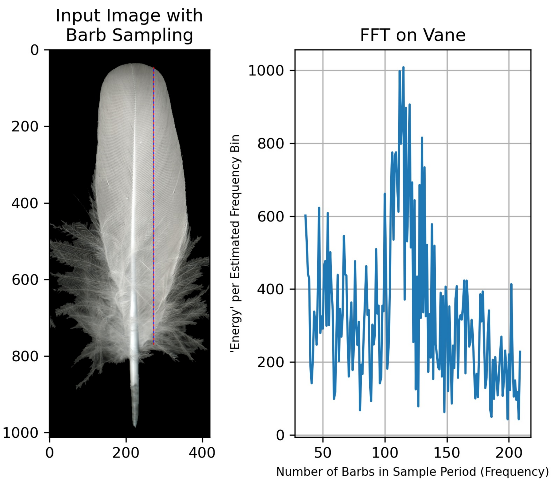

Fig. 3: An input image with barb sampling drawn based on density (red and blue sections) within a vane (left) and a plot of corresponding FFT values used for counting the barbs and ultimately their density within the vane (right).

Fig. 4: Tracing barbs on different feathers by cross-correlating pixel windows.

and image resolution may be controlled, as well as using the shape of the shaft to guide the image sampling, accurate results should be attainable. In lower-resolution images, manually assisted selection of feather image segments where barbs are visually distinct could also be used to improve accuracy.

Another aspect of feather analysis introduced is a first step towards extracting parametric curves to guide the path of barbs within a vane is shown in Figure 4 as tracing barbs via cross-correlation of pixels. We believe this to be the first published work to extract and parameterize these curves.

Figure 7 is a render of procedurally generated feather geometry following the approach of [20]. It is achieved by creating many curve instances to represent the substructures of a feather with calculations on orientation and position based on input such as guiding curves, barb and barbule densities and angles, and metadata from the Feather Atlas. The visual analysis presented in this study will continue to improve physically based geometric modeling of feathers based on real-world data rather than user estimation. Such techniques may also be applied to finding patterns in feather structure in order to be applicable in multiple fields of study such as paleontology. One such area of interest is investigating the appearance of fossilized feathers.

Applying the FFT technique to higher resolution and additional SEM images may be used for identifying barb subcomponents and estimating the barbule density along the length of a barb. The spacing currently approximated with FFT between barbs along the shaft based on normal-scale photography

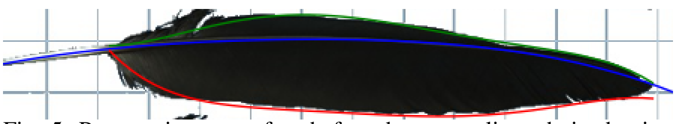

Fig. 5: Parametric curves for shaft and vane outlines derived using curve regression and drawn over the input image.

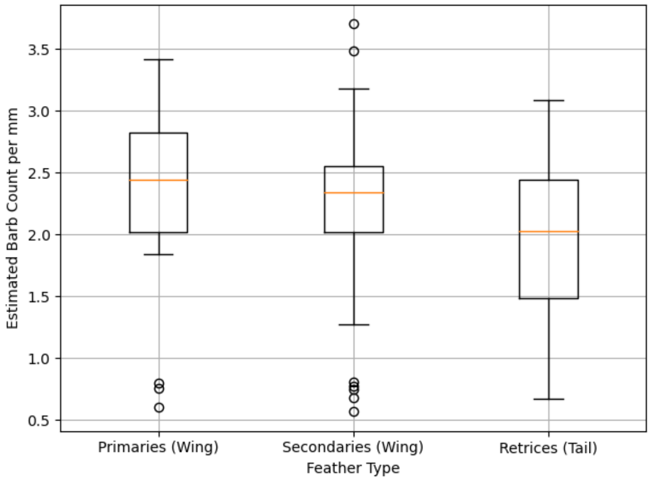

Fig. 6: Barb density as barbs per millimeter along the vane of 102 feather samples, separated by feather type. The values are approximated by FFT analysis.

includes the ramus and barbule substructures. The procedural generation of feathers for computer-graphics applications can be improved with continuing to build upon these methods as well. A high-quality photo of a specific type of feather may be used as the input, extracting shape properties (such as barb and barbule densities, angles, and guide curves) via image processing, and using these properties as parameters to drive the creation of highly accurate geometry for rendering. Another area of future work is generating accurate layouts of multiple feathers rather than a single feather, driven by visually analyzed statistics collected on all feather types and their placement in respect to one another on specific organisms.

Lastly, future work involves further processing of available images to refine the proposed data collection; collecting higher-resolution images of particular, representative specimens; and incorporating the extracted data into a procedural feather-generation pipeline.

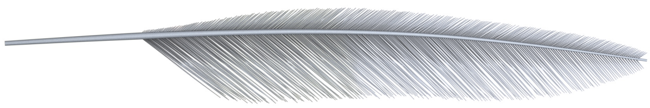

Fig. 7: Example of a feather procedurally generated using information derived from techniques presented in this paper.

References

[1] T. Hanson, *Feathers: The Evolution of a Natural Miracle*. Basic Books, 2011.

[2] A. C. Chandler, *A study of the structure of feathers, with reference to their taxonomic significance*. Berkeley, University of California press, 1916, vol. v.13:no.11 (1916). [Online]. Available: https://www.biodiversitylibrary.org/item/51770

[3] P. Trail, "The feather atlas," 2015. [Online]. Available: https://www.fws.gov/lab/featheratlas/

[4] D. Scott and C. McFarland, *Bird Feathers*, ser. A Guide to North American Species. Stackpole Books, 2010.

[5] T. Feo, D. Field, and R. Prum, "Barb geometry of asymmetrical feathers reveals a transitional morphology in the evolution of avian flight," *Proceedings in Royal Society B*, 2015.

[6] T. J. Feo and R. O. Prum, "Theoretical morphology and development of flight feather vane asymmetry with experimental tests in parrots," *Journal of Experimental Zoology*, vol. 322B, pp. 240–255, 2014.

[7] A. M. Rijke, "The water repellency and feather structure of cormorants, phalacrocoracidae," *Journal of Experimental Biology*, 1968.

[8] C. H. Greenewalt, *Hummingbirds*. Doubleday, 1960.

[9] J. Broggi, A. Gamero, E. Hohtola, M. Orell, and J.-Å. Nilsson, "Interpopulation variation in contour feather structure is environmentally determined in great tits," *PLoS One*, vol. 6, no. 9, 09 2011.

[10] G. Osvath, O. Vincze, D.-C. David, L. J. Nagy, A. Z. Lendvai, R. L. Nudds, and P. L. Pap, "Morphological characterization of flight feather shafts in four bird species with different flight styles," *Biological Journal of the Linnean Society*, vol. 131, no. 1, pp. 192–202, 07 2020. [Online]. Available: https://doi.org/10.1093/biolinnean/blaa108

[11] Y. Chen, Y. Xu, B. Guo, and H.-Y. Shum, "Modeling and rendering of realistic feathers," in *Proceedings of the 29th Annual Conference on Computer Graphics and Interactive Techniques*, ser. SIGGRAPH '02. New York, NY, USA: ACM, 2002, pp. 630–636.

[12] C. G. Franco and M. Walter, "Modeling and rendering of individual feathers," in *Proceedings of the 15th Brazilian Symposium on Computer Graphics and Image Processing*, ser. SIBGRAPI '02. Washington, DC, USA: IEEE Computer Society, 2002, pp. 293–299.

[13] L. Streit and W. Heidrich, "A biologically-parameterized feather model," in *Eurographics 2002*, vol. 21, no. 3. The Eurographics Association and Blackwell Publishers, 2002.

[14] D. Heckenberg, D. Gray, B. Smith, J. Wills, and C. Bone, "Quill: Birds of a feather tool," in *ACM SIGGRAPH 2011 Talks*, ser. SIGGRAPH '11. New York, NY, USA: ACM, 2011, pp. 34:1–34:1.

[15] W. Choi, N. Kim, J. Jang, S. Kim, and D. Yang, "Build your own procedural grooming pipeline," in *ACM SIGGRAPH 2017 Talks*, ser. SIGGRAPH '17. New York, NY, USA: ACM, 2017, pp. 54:1–54:2.

[16] R. Haapaoja and C. Genzwürker, "Mesh-driven generation and animation of groomed feathers," in *ACM SIGGRAPH 2019 Talks*, ser. SIGGRAPH '19. New York, NY, USA: Association for Computing Machinery, 2019. [Online]. Available: https://doi-org.libproxy.clemson.edu/10.1145/3306307.3328178

[17] N. Augello, D. Tonnesen, and A. Somasundaram, "Hummingbird: Dreamworks feather system," in *ACM SIGGRAPH 2019 Talks*, ser. SIGGRAPH '19. New York, NY, USA: Association for Computing Machinery, 2019. [Online]. Available: https://doi-org.libproxy.clemson.edu/10.1145/3306307.3328177

[18] X. Yan, B. Yang, W. Zhang, C. Liu, and Y. Wang, "An improved denoising algorithm of feather and down image based on ksvd," in *2016 8th International Conference on Information Technology in Medicine and Education (ITME)*, Dec 2016, pp. 419–423.

[19] H. Yue, K. Cai, B. Luo, Y. Jin, and Z. Zeng, "Denoising and segmentation of digital feather image using mean shift algorithm," 2015.

[20] J. Baron and E. Patterson, "Procedurally generating biologically driven feathers," in *Advances in Computer Graphics*. Springer International Publishing, 2019, pp. 342–348.

[21] L. C. Straker, "Quantitative characterization and comparative study of feather melanosome internal morphology using surface analysis," *Micron*, vol. 82, pp. 17 – 24, 2016. [Online]. Available: http://www.sciencedirect.com/science/article/pii/S0968432815300652

[22] C. M. Eliason, "Mechanisms and evolution of iridescent feather colors in birds," Ph.D. dissertation.